Journal of Power Sources 240 (2013) 390–396

Contents lists available at SciVerse ScienceDirect

Journal of Power Sources

journal homepage: www.elsevier.com/locate/jpowsour

The use of mixed carbon materials with improved oxygen transport in a lithium-air battery

Yining Zhang [a], Huamin Zhang [a,*], Jing Li [a,b], Meiri Wang [a], Hongjiao Nie [a,b], Fengxiang Zhang [a]

[a] Energy Storage Division, Dalian Institute of Chemical Physics, Chinese Academy of Sciences, Dalian 116023, China
[b] Graduate School of the Chinese Academy of Sciences, Beijing 100039, China

HIGHLIGHTS

- Super P exhibits better use of electrode space than KB600.
- Moderate wettability and hardly blocked pores promote gas transfer for Super P.
- Due to facilitated oxygen transfer, the capacity of mixed carbon is improved.

GRAPHICAL ABSTRACT

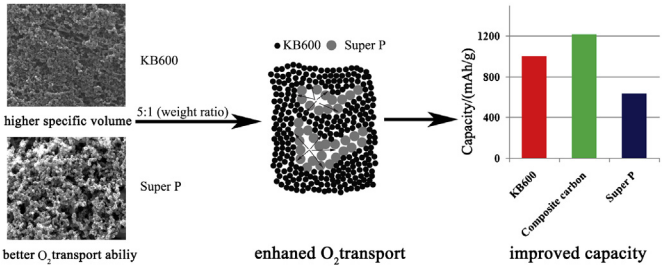

ARTICLE INFO

Article history:
Received 24 November 2012
Received in revised form
21 February 2013
Accepted 6 April 2013
Available online 18 April 2013

Keywords:
Lithium/air battery
Carbon material
Electrode structure
Oxygen transport
Porosity

ABSTRACT

Two commercial carbon blacks, Ketjen black EC600JD (KB600) and Super P with quite different porosity parameters, are used for the cathode of a lithium-air battery. With high specific pore volume, KB600 shows a higher weight specific capacity. However, Super P exhibits a super high volume specific capacity, about 7 times higher than that of KB600, ascribed to its higher proportion of pores with suitable size for the deposition of solid products. The effects of O_2 partial pressure and discharge rate on the specific capacity are investigated, combined with characterizations of contact angle and the structure of the electrodes. It is demonstrated that the Super P electrode possesses better O_2 transport that improves the use of the whole electrode volume, and the special mechanism of O_2 diffusion in the Super P electrode is proposed. By mixing KB600 with Super P with a weight ratio of 5:1, an electrode is obtained that exhibits increased O_2 transport. The weight specific capacity is 1219 mAh g^{-1}, about 1.2 times higher than that of KB600.

1. Introduction

The non-aqueous lithium-air/oxygen battery has been attracting more and more interests ascribed to its potential applications as energy conversion systems for various equipments, such as mobile devices, high attitude aircrafts and electric vehicles. Using lithium and oxygen as active materials for anode and cathode respectively, the battery exhibits a super high energy density, about 11,000 kWh kg^{-1}, or 5.5 kWh kg^{-1} if the oxygen is taken into account. However, to be commercialized, there are many obstacles to overcome, such as low rate discharge performance, low charge–discharge energy efficiency and poor cycle life [1,2]. Especially, the detailed charge–discharge reaction process is still unclear, and much work has to be done to make it operate as a rechargeable battery [3–6]. Thus, it might be an achievable target to use it as a primary battery with a super high capacity in the near future.

Same as other metal-air batteries, the oxygen reduction reaction (ORR) of a lithium-air battery takes place in the cathode, which is

* Corresponding author. Fax: +86 411 84665057.
E-mail address: zhanghm@dicp.ac.cn (H. Zhang).

0378-7753/$ – see front matter © 2013 Elsevier B.V. All rights reserved.
http://dx.doi.org/10.1016/j.jpowsour.2013.04.018

also named as the "air breathing electrode" because the oxygen could be directly obtained from air. Such reaction should occur on the solid–liquid interface formed by the electrode material and the electrolyte so that the charge transfer process involving the electron and the Li^+ can be facilitated. More surface area of the electrode material covered by the electrolyte will provide more interface for the ORR reaction. However, different from traditional metal-air batteries using aqueous electrolyte, the reduced oxygen is combined with Li^+ to form the solid lithium oxide, and the product is insoluble in the organic electrolyte. Therefore, the solid–liquid interface is responsible for both the electrochemical reaction and the deposition of the solid product. As the reaction goes on, the lithium oxides gradually accumulate in the pores of the electrode material, and the discharge process will terminate when the pores are completely filled.

The above analysis implies that the capacity is determined by the available surface for the deposition and the pore volume for the storage of solid products. Large surface area and pore volume are definitely desirable [7], but the pores size distribution (PSD) of the electrode material also plays an important role [8]. At the beginning of the discharge, the micropores and some of the mesopores with smaller size than that of the lithium oxide particles would be easily blocked, and will not be further accessed by either oxygen or Li^+, making them unavailable; in contrast, for the pores with too large size, the growing lithium oxide layer with low conductivity will make the polarization of the electrochemical reaction higher and thus, the discharge process would end before the whole pore volume is occupied. Therefore, the mesopores with appropriate size, e.g. tens of nm, is favorable to obtain a high use, and the synthesis of various carbon materials with a high proportion of mesopores is important for the lithium-air battery [9,10].

On the other hand, since the reaction takes place at the solid–liquid interface as mentioned above, O_2 should be dissolved in the electrolyte and diffuses to the interface to participate in the reaction. Therefore, the solubility and the diffusion rate of O_2 would have significant impacts on the reaction [11,12]. It is confirmed that an appropriate choice of the electrolyte and increasing the O_2 partial pressure are effective strategies to improve the solubility and can achieve increased O_2 transport in the electrode [13]. Meanwhile, intelligent designs of the pore architecture and the electrode structure could also promote the transport [14,15]. For example, Williford and Zhang [16] proposed an interconnected dual-pore structured electrode, where pores with high ORR activity allow for the deposition of products, and the other pores with low or no activity will remain open for the O_2 access. Another feasible solution is to modify the configuration of the electrode with supporting materials [17,18], such as Ni foam and carbon cloth, which can form open and interconnected three-dimensional (3D) channels; by this means, the active materials, such as carbon blacks (CBs), carbon nanofibers, are supported on the framework of supporting materials, so that an efficient O_2 transport as well as a high Li^+ migration rate can be obtained, which is favorable for the high capacity and rate discharge performance.

It is now clear that a better use of the pores of electrode materials requires appropriate PSDs, and for a better use of the whole electrode volume, efficient O_2 transport is necessary. Normally, commercial Ketjen black EC600JD (KB600) [19,20] is used as the cathode material ascribed to its high specific volume, in order to obtain a high discharge capacity. Super P [21–23], whose specific volume and surface area are both quite low, has also been used, and can produce a relatively high performance. In order to better understand the factors influencing the use of the electrode volume and achieve an optimal battery performance, we herein studied both KB600 and Super P as the cathode materials with different porosity parameters, by carrying out systematic pores structure characterizations combined with discharge tests at different conditions. We also proposed an O_2 transport mechanism in the electrodes fabricated using different CBs. Finally, with the understanding on the unique property of Super P in the O_2 transport, we fabricated a novel composite cathode comprising KB600 and Super P with a selected ratio, and examined its feasibility in improving the discharge capacity.

2. Experimental

2.1. Materials and characterizations

Commercial CBs, KB600 (AkzoNobel) and Super P (TIMCAL) were purchased and directly used for cathode preparations without further treatments. The analysis of nitrogen adsorption–desorption isotherms was carried out to measure the porosity of the CBs by an ASAP 2420 adsorption analyzer (Micromeritics). The Brunauer–Emmett–Teller (BET) method was used for the surface area measurement. The Barrett–Joyner–Halenda (BJH) adsorptions–desorption was used for the pore analysis. The total pore volume was calculated from the adsorbed volume of nitrogen at $P/P_0 = 0.99$ (saturation pressure). PSDs were obtained by the BJH method from the desorption branches of the isotherms. All the results were related to the pores between 1.7 nm and 300 nm.

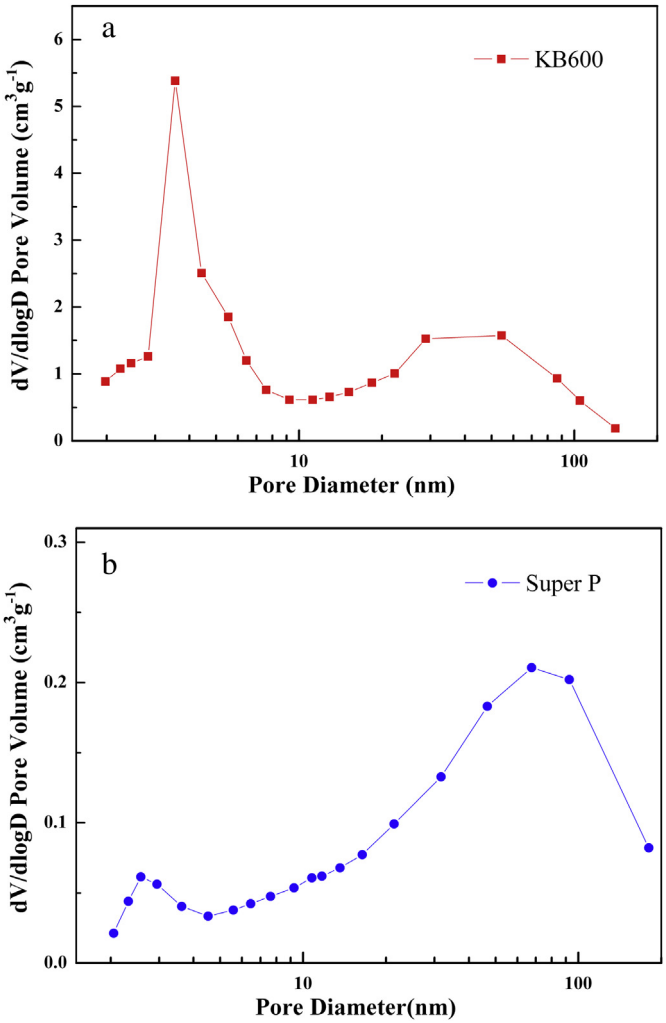

Fig. 1. PSDs of the CBs (a) KB600 [25], (b) Super P.

Table 1
Porosity parameters of the CBs (diameter: 1.7–300 nm).

Material	S_{BET} ($m^2\ g^{-1}$)	V_{total}[a] ($cm^3\ g^{-1}$)	V_A[a] ($cm^3\ g^{-1}$)	V_B[a] ($cm^3\ g^{-1}$)
KB600	1379	2.61	1.35 (52%)	1.26 (48%)
Super P	54	0.23	0.03 (13%)	0.20 (87%)

[a] V_A, V_B stand for the volume of Pore A (diameter < 10 nm) and Pore B (10 nm < diameter < 300 nm) respectively; the data for KB600 is cited from reference [25].

2.2. Preparations of electrodes and characterizations

To make gas diffusion electrodes, the CBs were mixed with polytetrafluorethylene (PTFE) (dry weight ratio of 8:2) in isopropanol. After drying in air, the slurry was rolled and cut into film electrodes with a carbon loading of 6.7 ± 0.4 mg cm^{-2}. The electrode structure was characterized by SEM tests using the JEOL JEM-5600LV operating at 20 kV. Furthermore, to evaluate the electrode wettability with the electrolyte, contact angle tests were also performed.

2.3. Fabrications and evaluations of single cells

The single cell was assembled in an argon-filled glove box, under a dry argon atmosphere with H_2O and O_2 levels less than 1.0 and 0.5 ppm respectively, using a stainless steel bar as the anode current collector, a lithium metal foil as the anode, a porous polypropylene separator soaked with electrolyte (1 M $LiPF_6$ in propylene carbonate and ethylene carbonate with weight ratio of 1:1), a disc of 1.6 cm diameter cathode electrode, a nickel mesh and a stainless steel spring on the top of it as the cathode current collector. The cell parts were compressed together to ensure that the electrode contact is good and then the cell was completely sealed except for two channels as the O_2 inlet and outlet.

Then, the cell was exposed to O_2 with a purity of 99.999% at certain pressure for a minimum of 3 h prior to the electrochemical tests, and all the measurements were carried out at room temperature. The electrochemical performance of the prepared cells was examined using a BT2000 cell test system by Arbin instruments. The discharge was conducted at a constant current with a cut-off voltage of 2.0 V.

3. Results and discussion

3.1. Porosity analysis of the CBs

Fig. 1 shows the PSDs of KB600 and Super P. Herein, 10 nm, similar to the size of the solid product particle [24], is set as the reference point, and roughly two regions can be identified: 1) Pore A (diameter < 10 nm) with a lower use of pores volume, 2) Pore B (10 nm < diameter < 300 nm) with a better use. For Pore A, diameters of the CBs both center at around 3–4 nm, and for Pore B, the diameter of Super P centers at around 70 nm, a little higher than that of KB600. Meanwhile, as shown in Table 1, the Pore B volume proportion of Super P is about 87%, much higher than that of KB600, which is about 48%. Thus, a better use of the total pores volume could be obtained using Super P, ascribed to its higher proportion of pores with appropriate size for the deposition of products. However, the Pore B volume of Super P is only 0.2 $cm^3\ g^{-1}$, about 16% of KB600. Furthermore, the Super P:KB600 ratio of V_{total} and S_{BET} is even much lower, about 1:11 and 1:26 respectively, indicating that KB600 would be a better candidate for the battery to obtain a higher weight specific capacity, although its utilization might be lower.

3.2. Structure characterizations of the electrodes before discharge

SEM tests were carried out to characterize the structure of the electrodes fabricated using the two CBs. Although the electrodes are both composed of spherical particles (Fig. 2), their pore

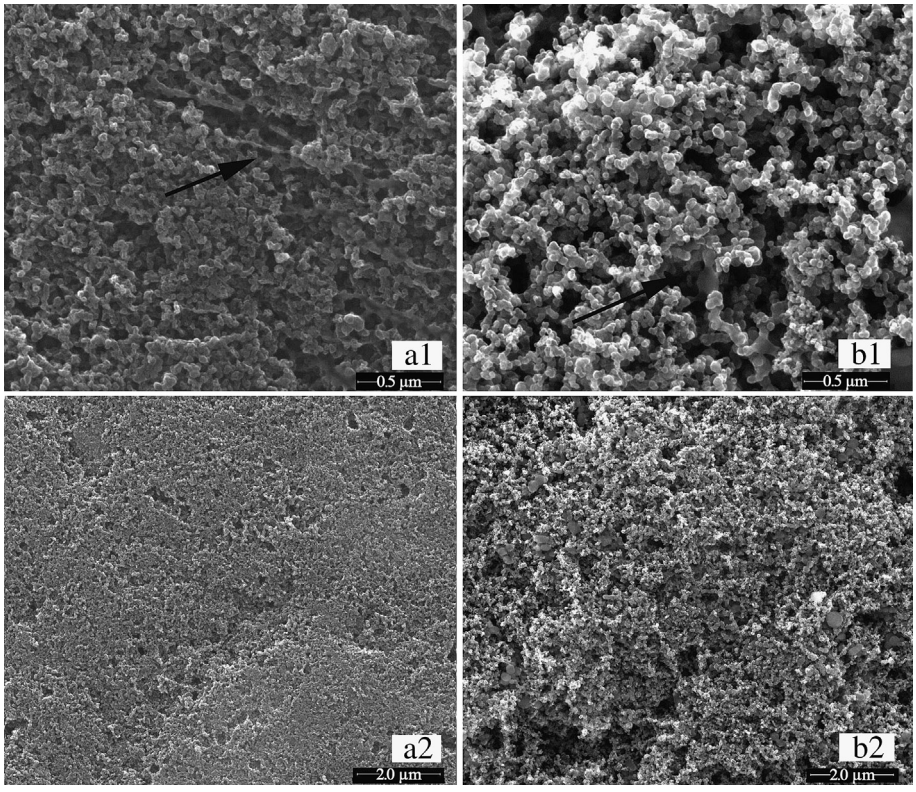

Fig. 2. Structure of the electrodes before discharge, a. KB600, b. Super P; a1 and b1 obtained at 100000×, a2 and b2 obtained at 25000×.

structures are quite different. Firstly, the particle size of Super P is about 40 nm, higher than that of KB600, which is about 20 nm. Larger particle size and lower Pore A proportion result in a lower BET surface area of Super P.

Secondly, although the electrodes both contain particle aggregates and two pores (one formed by the interstices among the single particles, and the other by the interstices among the aggregates), the KB600 particles accumulate closely to form large aggregations, making the electrode quite compact, while the Super P electrode obviously appears much looser, especially at the high magnification. There seems to be a repulsion force among the Super P particles to prevent them attaching to each other, which is different from the case of Kb600. It's well known that the surface of the carbon material is reach in various oxygen groups, whose type and amount vary according to the synthesis process of the carbon material. The rich surface groups greatly affect the chemical and physical properties of the material, such as electronic property and wettability with various solvent. Different surface properties of the two CBs might cause the difference in the interactions between the carbon particles. The larger particle size and the repulsion make the interstices among the Super P particles much larger, agreeing well with the analysis of PSDs in part 3.1. Additionally, the Super P aggregates with relatively small size exist in a different way, connecting with each other like branches to form a 3D framework. The electrode possesses numerous large interconnected pores, about hundreds of nm. The difference in the pore structure will cast a great impact on the discharge capacity through influencing the product depositions and the O_2 transport.

Lastly, the binders in the electrodes also show different morphology, marked by the arrows as shown in Fig. 2a1 and b1 respectively. For KB600 electrode, the binder is highly dispersed and stretched into line shape, which might be due to the repeated rolling press process in the electrode fabrication. For Super P electrode, isolated solid bulks of PTFE can be found, indicating its worse compatibility with Super P than with KB600, which should be also caused by their different surface properties.

3.3. Evaluations of specific capacities

Discharge tests were carried out to evaluate the performance of single cells. As shown in Fig. 3, the KB600 electrode yielded a higher specific capacity, which was expected based on the porosity analysis. The results are 1005 mAh g^{-1} and 635 mAh g^{-1} for KB600 and Super P respectively. However, if the specific pore volumes of the two CBs are considered, the use of the whole electrode volume shows opposite results. As shown in Table 2, the volume specific capacity of Super P is 2761 mAh cm^{-3}, about 7 times higher than that of KB600. The analysis of BET results indicated that higher proportion of Pore B could improve the use of the electrode volume. Furthermore, considering that the Pore A shows lower use for the deposition of solid products, the volume specific capacities were recalculated based on Pore B; this time, the value for Super P is 3175 mAh cm^{-3}, about 4 times higher than that of KB600. Therefore, in addition to PSDs, there are still other factors that contribute to the better use of the electrode volume of Super P.

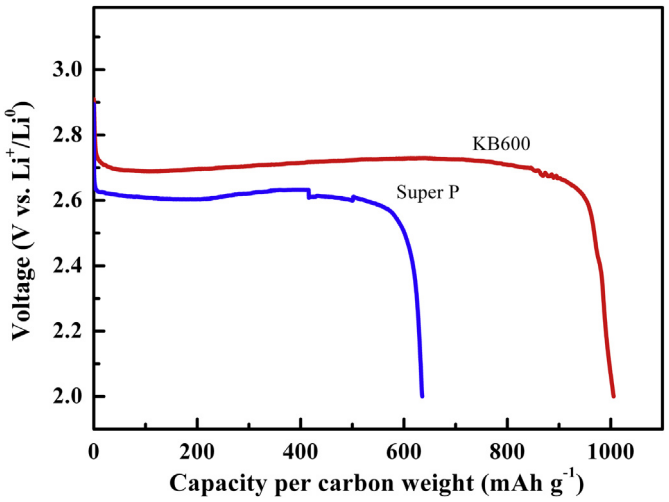

Fig. 3. Weight specific capacity discharged at 30 mA g^{-1} carbon, 1 atm O_2.

Table 2
Specific capacity of the CBs.

Material	Weight specific capacity (mAh g^{-1})	[a] Volume specific capacity (mAh cm^{-3})	[b] Volume specific capacity (mAh cm^{-3})
KB600	1005	385	798
Super P	635	2761	3175

[a] a and b stand for results considering the total volume and the volume of Pore B (10 nm < diameter < 300 nm) respectively.

3.4. Effects of the O_2 partial pressure and the discharge rate on the capacity

The effects of experiment conditions on the cell performance were also investigated, as shown in Fig. 4. Firstly, as the O_2 partial pressure is increased to 2.5 atm from 1 atm, the specific capacities are increased for both the electrodes. It's well known that the O_2 solubility could be increased through the improvement of its partial pressure, which can facilitate its transport in the electrode. Since the O_2 solubility shows greater impact on KB600 than that on Super P, it can be inferred that the gas transport in the KB600 electrode is worse. Secondly, as the current density is increased to 60 mA g^{-1} from 30 mA g^{-1}, the specific capacities both decrease. The retention rate of Super P is higher, indicating that it possesses better rate discharge performance. In order to explore the reasons for the above differences, further characterizations of the electrodes were performed as follows.

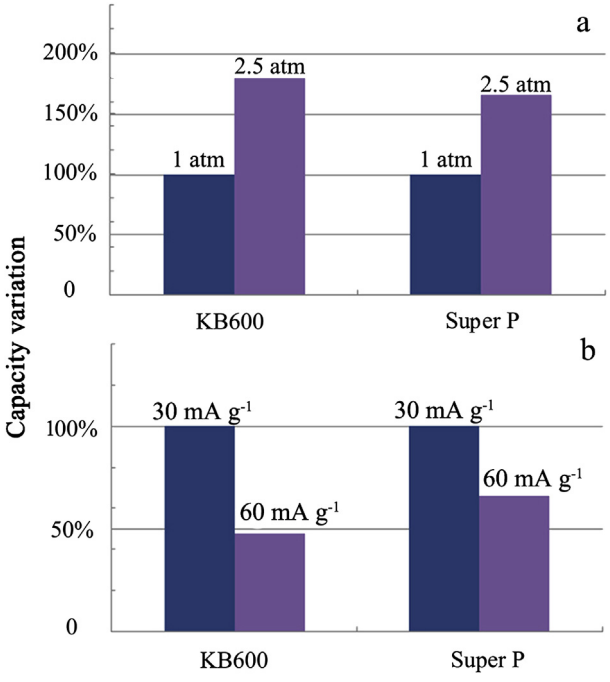

Fig. 4. Effects of discharge conditions on the capacity, a. O_2 partial pressure, b. current density.

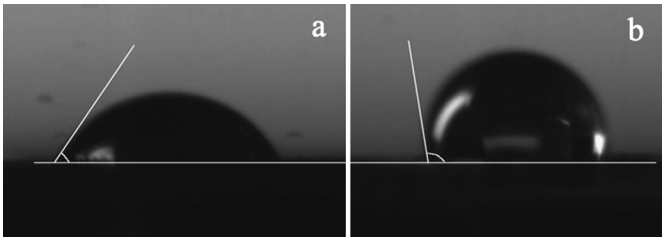

Fig. 5. Contact angle tests, a. KB600, b. Super P.

3.5. Contact angles tests

The compatibility of the electrode material with the electrolyte shows significant effect on the formation of the solid–liquid reaction interface. Normally, more pores soaked up by the electrolyte will mean more volume for the electrochemical reaction and the accumulation of products. However, that will meanwhile increase the resistance of the O_2 transport in the electrode due to its low solubility in the non-aqueous electrolyte. Wettability tests were taken to evaluate the compatibility, as shown in Fig. 5. The contact angle for KB600 electrode is 56°, lower than that for Super P, which is 99°. This difference might be also caused by their different surface properties. Additionally, the dispersion state of PTFE in the electrode may also affect the wettability. Due to its lyophilic character, the KB600 electrode suffers from lower O_2 transport rate in water-flood like situation, especially in the case of discharge at high rate with thick electrode, where the mass transport is the dominant factor. In contrast, ascribed to its lyophobic character, there is a certain amount of pores without the electrolyte infiltrating in the Super P electrode, acting as the highway for O_2 transport.

3.6. Structure characterizations of the electrodes after discharge

To find out how the discharge products deposited on the cathode, we disassembled the battery after discharge and examined the electrode structures under SEM. Similar to the comparison before

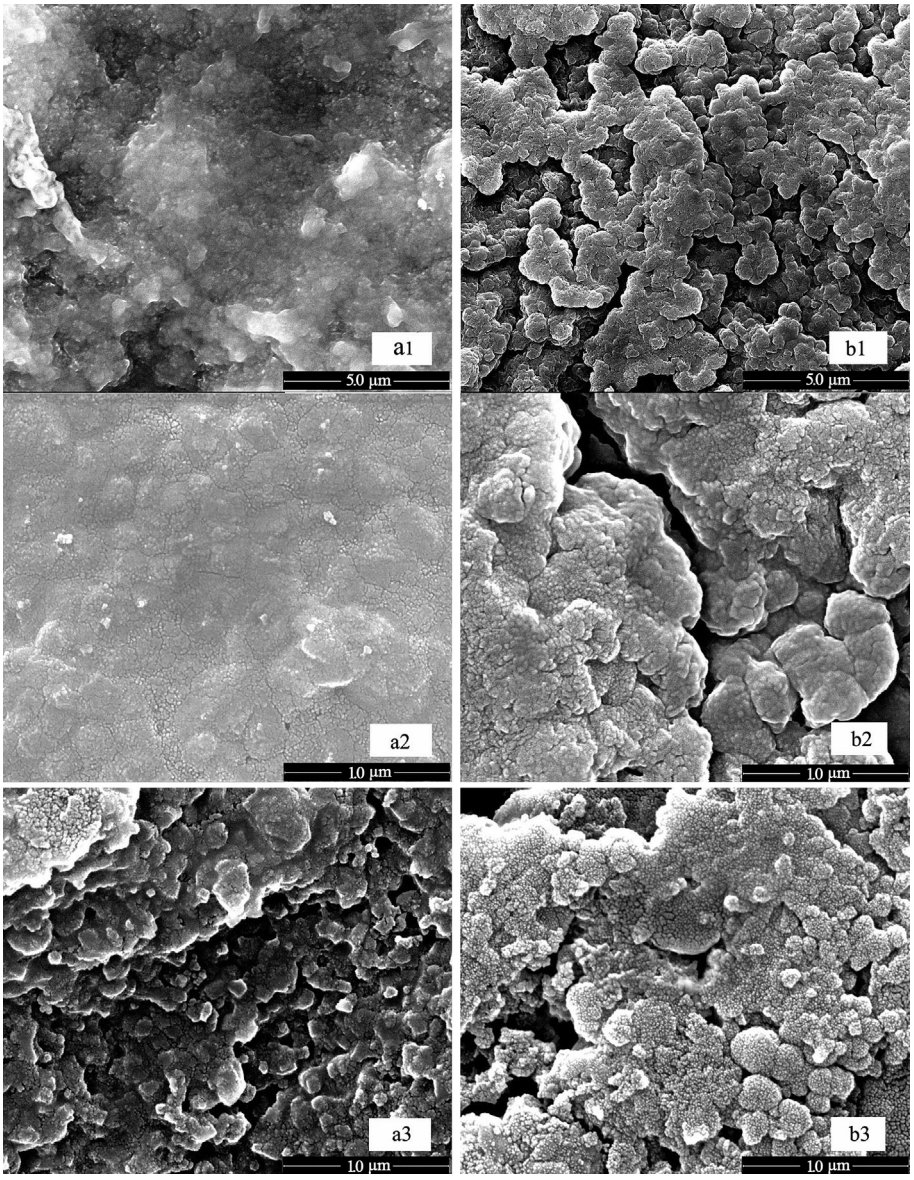

Fig. 6. Morphology of the electrodes after discharge, a. KB600, b. Super P; 1 and 2 for the side facing the O_2 inlet at 20000× and 100000× respectively; 3 for the side facing the membrane side at 100000×.

discharge, the electrodes of KB600 and Super P display quite differently. For KB600 electrode, the pores are fully filled with the solid products at the side facing the oxygen inlet named as external side (Fig. 6a1 and a2), while at the side facing the membrane named as internal side, there are many pores left empty, which could still be used for the deposition of products (Fig. 6a3). These observations demonstrate that the use of the internal electrode volume is far below that of the external side. To participate in the reaction, O_2 should be delivered through the pores from the external side to the internal side. Longer transport distance means higher resistance for the gas transport, and the discharge products tend to deposit at the external side with more sufficient O_2 supply. Once the external pores are filled up, the inlets for the O_2 to diffuse into the electrode will be blocked, leaving the internal pores insufficiently availed.

For the Super P electrode, the pores with the size of hundreds of nm formed by the particle aggregations can't be filled up during discharge due to their large size. However, that means it's difficult to block those pores. As shown in Fig. 6b1 and b2, the cracks at the external side after discharge indicate that a certain amount of pores keeps open in the whole discharge process, which can act as the O_2 transport ways for the internal pores of the electrode. Fig. 6b3 shows the occupation of internal electrode, and compared with the Fig. 6b2, the accumulation density of products is a little lower. However, the gap is much lower than that in the case of the KB600 electrode, evidencing that the Super P electrode possesses better O_2 transport.

3.7. Analysis of factors influencing the capacity

Based on the electrode structure characterizations and the contact angle tests, the results of discharge capacities at different conditions can be explained as follows. Firstly, the Super P electrode has better mass transfer because of its moderate compatibility with the electrolyte and hardly blocked pore structure, and therefore can achieve better use of the internal pores as well as better use of the whole electrode volume. Additionally, the effect of O_2 partial pressure corresponding to its solubility in the electrolyte on the capacity can be decreased.

Secondly, the KB600 features water-flood like electrode and easily blocked pores structure, which results in low use of the whole electrode volume, and makes it rely more on the improvement of the O_2 partial pressure to promote the transfer process. For the same reason, higher the discharge rate is, more easily the external side could be blocked, resulting in lower capacity retention as the current increases. While for Super P electrode, the open pores in the external side are beneficial for obtaining a better rate discharge performance.

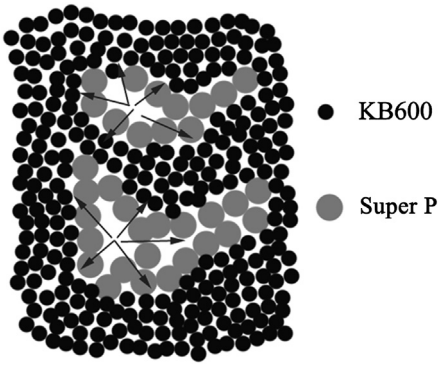

Fig. 7. Diagram of the electrode fabricated using the mixed carbon material.

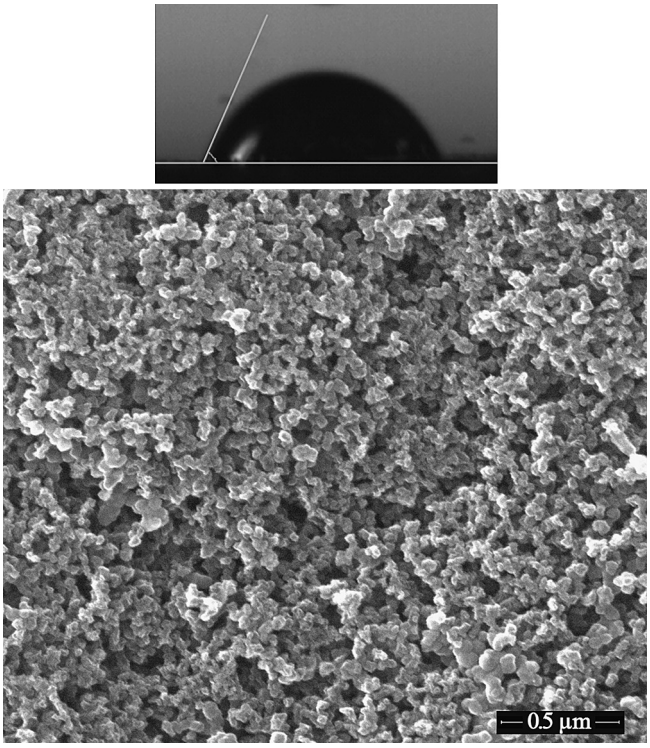

Fig. 8. Contact angle test and structure characterization with the electrode fabricated using the mixed carbon material.

3.8. The mixed carbon material with better O_2 transport

In order to combine the advantages of the two CBs, we prepared a novel electrode material by mixing KB600 with Super P at a weight ratio of 5:1, as shown in Fig. 7. Besides the function for the electrochemical reaction and the deposition of products, Super P provides O_2 transport ways with large pores, through which O_2 diffuses all around. As shown in Fig. 8, the two CBs are well mixed in the obtained electrode, and the addition of Super P has changed the gathering state of KB particles. Compared with the pure KB electrode, the particle aggregation size is reduced, and the electrode seems relatively loose. Table 3 lists the corresponding electrode porosity parameters. Due to the addition of Super P, the surface area, the total specific volume and the volumes in the special regions have been reduced. However, the proportion of Pore B is increased and larger than that of Pore A, indicating a modified PSD. Furthermore, the contact angle of the obtained electrode is increased to 67° as shown in Fig. 8, and the decreased lyophilic character is beneficial to improve gas transport in the electrode. In order to examine the effect, discharge test is carried out and the result shows that the specific capacity is 1219 mAh g^{-1}, higher than both KB600 and Super P. Additionally, the volume specific capacity based on the total volume is 570 mAh cm^{-3}, which is about 1.5 times higher than that of KB, indicating an increased space utilization. Aided by Super P to promote the O_2 diffusion, the property of high specific volume of KB600 is made better use of, and the capacity is improved.

Table 3
Porosity parameters of the mixed carbon material (diameter: 1.7–300 nm).

S_{BET} (m^2 g^{-1})	V_{total} (cm^3 g^{-1})	V_A[a] (cm^3 g^{-1})	V_B[a] (cm^3 g^{-1})
1122	2.14	1.06 (49.5%)	1.08 (50.5%)

[a] V_A, V_B stand for the volume of Pore A (diameter < 10 nm) and Pore B (10 nm < diameter < 300 nm) respectively.

4. Conclusion

Appropriate PSD is beneficial to obtaining a better use of the pore volume of the carbon material for the lithium-air battery in regard to accumulations of solid products in the pores. However, the factor of O_2 transport should be taken into account to obtain a better use of the whole electrode volume, which is of practical importance. Ascribed to its suitable wettability with the electrolyte, the electrode of Super P could obtain the balance between solid–liquid reaction interface area and pores for the O_2 transport. Furthermore, a certain amount of large pores is necessary to keep O_2 transport paths, since the pores can't be blocked in the whole discharge process due to their low volume use. For KB600, the high specific volume makes it a competitive candidate. However, how to make good use of the pores remains a big challenge. One proposed solution is to change its compatibility with the electrolyte, either by electrolyte selection or by the modification of the surface property. In addition, making the electrode looser and formation of large pores are worthy of the further attempt, through altering the interactions among the particles. In this work, Super P as the additive was mixed with KB600 to prepare the electrode with improved mass transport, and a higher specific capacity was achieved.

Acknowledgment

Thanks Dong Mingquan and Pan Bo a lot for their constructive suggestions and help on the design of single cell and corresponding performance evaluation.

References

[1] R. Padbury, X. Zhang, J. Power Sources 196 (2011) 4436–4444.
[2] G. Girishkumar, B. McCloskey, A.C. Luntz, S. Swanson, W. Wilcke, J. Phys. Chem. Lett. 1 (2010) 2193–2203.
[3] J. Xiao, J. Hu, D. Wang, D. Hu, W. Xu, G.L. Graff, Z. Nie, J. Liu, J.-G. Zhang, J. Power Sources 196 (2011) 5674–5678.
[4] X. Ren, S.S. Zhang, D.T. Tran, J. Read, J. Mater. Chem. 21 (2011) 10118–10125.
[5] B.D. McCloskey, D.S. Bethune, R.M. Shelby, G. Girishkumar, A.C. Luntz, J. Phys. Chem. Lett. 2 (2011) 1161–1166.
[6] S.A. Freunberger, Y. Chen, Z. Peng, J.M. Griffin, L.J. Hardwick, F. Barde, P. Novak, P.G. Bruce, J. Am. Chem. Soc. 133 (2011) 8040–8047.
[7] P. Kichambare, J. Kumar, S. Rodrigues, B. Kumar, J. Power Sources 196 (2011) 3310–3316.
[8] C. Tran, X.Q. Yang, D.Y. Qu, J. Power Sources 195 (2010) 2057–2063.
[9] X.H. Yang, P. He, Y.Y. Xia, Electrochem. Commun. 11 (2009) 1127–1130.
[10] M. Mirzaeian, P.J. Hall, Electrochim. Acta 54 (2009) 7444–7451.
[11] S.S. Sandhu, J.P. Fellner, G.W. Brutchen, J. Power Sources 164 (2007) 365–371.
[12] J. Read, K. Mutolo, M. Ervin, W. Behl, J. Wolfenstine, A. Driedger, D. Foster, J. Electrochem. Soc. 150 (2003) A1351–A1356.
[13] X.H. Yang, Y.Y. Xia, J. Solid State Electrochem 14 (2010) 109–114.
[14] J. Xiao, D. Mei, X. Li, W. Xu, D. Wang, G.L. Graff, W.D. Bennett, Z. Nie, L.V. Saraf, I.A. Aksay, J. Liu, J.-G. Zhang, Nano Lett. (2011) 5071–5078.
[15] Y. Li, J. Wang, X. Li, D. Geng, R. Li, X. Sun, Chem. Commun. 47 (2011) 9438–9440.
[16] R.E. Williford, J.G. Zhang, J. Power Sources 194 (2009) 1164–1170.
[17] S.D. Beattie, D.M. Manolescu, S.L. Blair, J. Electrochem. Soc. 156 (2009) A44–A47.
[18] H.-G. Jung, J. Hassoun, J.-B. Park, Y.-K. Sun, B. Scrosati, Nat. Chem. 4 (2012) 579–585.
[19] J.G. Zhang, D.Y. Wang, W. Xu, J. Xiao, R.E. Williford, J. Power Sources 195 (2010) 4332–4337.
[20] J. Xiao, D.H. Wang, W. Xu, D.Y. Wang, R.E. Williford, J. Liu, J.G. Zhang, J. Electrochem. Soc. 157 (2010) A487–A492.
[21] S.S. Zhang, K. Xu, J. Read, J. Power Sources 196 (2011) 3906–3910.
[22] J. Read, J. Electrochem. Soc. 149 (2002) A1190–A1195.
[23] S.A. Freunberger, Y. Chen, N.E. Drewett, L.J. Hardwick, F. Barde, P.G. Bruce, Angew. Chem. Int. Ed. 50 (2011) 8609–8613.
[24] R. Black, S.H. Oh, J.-H. Lee, T. Yim, B. Adams, L.F. Nazar, J. Am. Chem. Soc. 134 (2012) 2902–2905.
[25] J. Li, H.M. Zhang, Y.N. Zhang, M.R. Wang, F.X. Zhang, H.J. Nie, Nanoscale (2013), http://dx.doi.org/10.1039/C3NR00337J.